

Quantification of Modeling Uncertainty in the Rayleigh Damping Model

Farid Ghahari^{1,*}, Khachik Sargsyan^{2,†}, Ertugrul Taciroglu^{1,‡}

¹ *Civil and Environmental Engineering Department, University of California, Los Angeles, CA 90095, USA*

² *Sandia National Laboratories, Livermore, CA 94550, USA*

ABSTRACT

Understanding and accurately characterizing energy dissipation mechanisms in civil structures during earthquakes is an important element of seismic assessment and design. The most commonly used model is attributed to Rayleigh. This paper proposes a systematic approach to quantify the uncertainty associated with Rayleigh's damping model. Bayesian calibration with embedded model error is employed to treat the coefficients of the Rayleigh model as random variables using modal damping ratios. Through a numerical example, we illustrate how this approach works and how the calibrated model can address modeling uncertainty associated with the Rayleigh damping model.

INTRODUCTION

Energy dissipation mechanisms in civil structures during an earthquake generally reduce the load demands on structural components. These mechanisms are typically classified into three types: structural inelasticity, energy radiation resulting from the interaction of the structure with the surrounding medium (e.g., soil), and inherent damping. While the first two sources of damping are well-studied and can be modeled with relatively good accuracy, inherent damping cannot be derived from first principles and fundamental structural/material properties [1]. Instead, phenomenological approaches are adopted (e.g., Rayleigh damping) to model this diffuse, and often elusive, type of damping. Although the importance of inherent damping is only marginal during strong events due to the larger contribution of inelastic behavior of structural components (materials) [2], it plays a crucial role in the performance of structures under operational conditions and/or frequent weak or moderate wind/earthquake events, especially in tall buildings [3].

Modal damping ratios identified from real-life data collected through field experiments [4] or weak seismic events [5–7] provide the most reliable approach for modeling inherent damping. However, the direct application of modal damping is generally limited to linear analyses and cannot be employed for conducting nonlinear time-history analysis. To that end, an equivalent damping matrix representing the inherent damping must be calculated using the identified modal damping ratios. One approach is to superpose modal damping matrices using normal mode shapes [8] as follows

$$\mathbf{C} = (\mathbf{\Phi}^T)^{-1} \tilde{\mathbf{C}} \mathbf{\Phi}^{-1}, \quad (1)$$

where \mathbf{C} and $\mathbf{\Phi}$ are $n \times n$ damping and normal mode shape matrices, respectively, and matrix $\tilde{\mathbf{C}}$ is defined as

$$\tilde{\mathbf{C}} = \begin{bmatrix} 2\xi_1 m_1 \omega_1 & & \mathbf{0} \\ & \ddots & \\ \mathbf{0} & & 2\xi_n m_n \omega_n \end{bmatrix}, \quad (2)$$

with modal mass, damping ratio, and undamped natural frequency denoted, respectively, as m_i , ξ_i , and ω_i , and n is the total Degrees-Of-Freedoms (DOFs) of the structure. However, there are two main problems with this approach. First, the matrix would not be band-limited like the mass and stiffness matrices, significantly increasing the computational burden. Second, modal damping ratios of all modes are needed; otherwise, it could lead to numerical instabilities when conditionally stable numerical integration schemes are used if zero values are assigned to the damping associated with the higher modes.

Due to the aforementioned issues, the most common damping model used for dynamic analysis is a viscous model originally proposed by Rayleigh (1898). This so-called Rayleigh damping assumes that the total inherent damping is a combination of the kinetic and potential energies, allowing the damping matrix to be represented as

* Research Scientist. Corresponding author: Farid Ghahari, E-mail: faridghahari@ucla.edu

† Research Scientist

‡ Professor.

$$\mathbf{C} = a_0 \mathbf{M} + a_1 \mathbf{K}, \quad (3)$$

where \mathbf{M} and \mathbf{K} are mass and stiffness matrices, respectively. The coefficients a_0 and a_1 are referred to as mass- and stiffness-proportional coefficients, respectively. Although numerous studies have been conducted to justify or evaluate this model [10–13], the main reason behind its popularity is its favorable mathematical features. First, it is determined by only two coefficients, so modal damping ratios at only two modes (i and j) are needed, as shown in Eq. (4).

$$\begin{bmatrix} a_0 \\ a_1 \end{bmatrix} = 2 \begin{bmatrix} 1/\omega_i & \omega_i \\ 1/\omega_j & \omega_j \end{bmatrix}^{-1} \begin{bmatrix} \xi_i \\ \xi_j \end{bmatrix}. \quad (4)$$

Second, the damping matrix is band-limited, which avoids an increase in computational costs. Third, mode shapes are orthogonal with respect to this damping matrix, still allowing the use of modal analysis of linear systems. Utilizing this model, modal damping ratios of other modes can be easily calculated as

$$\xi_k = \frac{a_0}{2\omega_k} + \frac{a_1}{2} \omega_k \quad \text{for } k = 1 \dots n. \quad (5)$$

Although a few numerical issues have been reported regarding the implementation of this damping model [14–17], it remains the primary model implemented in most analysis software [18,19]. Consequently, numerous studies have been devoted to determining which modes should be used for calculating the coefficients a_0 and a_1 [16].

As discussed above, the Rayleigh damping model is essentially a simplified model aimed at facilitating the dynamic analysis of structures without a first-principle basis. Consequently, modal damping ratios calculated using Eq. (5) could significantly differ from true values. For example, several studies suggest that a mass-proportional component does not make physical sense, and damping ratios inferred from instrumented buildings follow a stiffness-proportional pattern more accurately [3,11,20]. While such discrepancies are generally accepted within the research and engineering community, this modeling uncertainty has rarely been quantified. This study proposes a systematic approach to quantify the uncertainty associated with the Rayleigh damping model by embedding the existing error between the Rayleigh model and true modal damping ratios into the coefficients a_0 and a_1 . In the present study, we consider these two parameters as random variables, enabling us to incorporate into response analyses both the estimation and modeling uncertainties corresponding, respectively, to the error in the identified modal damping ratios and the discrepancy between these values and the Rayleigh model.

RAYLEIGH MODEL CALIBRATION

In this study, we employ the Bayesian calibration technique [21] to estimate the parameters of the Rayleigh model, denoted as $\boldsymbol{\theta} = [a_0 \ a_1]^T$, using a set of identified modal damping ratios, $\hat{\boldsymbol{\xi}}(\boldsymbol{\omega}) = [\hat{\xi}_1 \ \dots \ \hat{\xi}_n]^T$, at n arbitrary natural frequencies, $\boldsymbol{\omega} = [\hat{\omega}_1 \ \dots \ \hat{\omega}_n]^T$. According to the Bayes theorem, the *posterior* Probability Density Function (PDF) of $\boldsymbol{\theta}$ given the measured data can be expressed as

$$p(\boldsymbol{\theta}|\hat{\boldsymbol{\xi}}) \propto p(\hat{\boldsymbol{\xi}}|\boldsymbol{\theta})p(\boldsymbol{\theta}) \quad (6)$$

where $p(\boldsymbol{\theta})$ is the prior PDF of the parameters, and $p(\hat{\boldsymbol{\xi}}|\boldsymbol{\theta})$ is the likelihood of the Rayleigh model's ability to explain measured data. Assuming the Rayleigh model is a perfect model, the identified and predicted damping ratios are related as

$$\hat{\boldsymbol{\xi}}(\boldsymbol{\omega}) = \boldsymbol{\xi}(\boldsymbol{\omega}; \boldsymbol{\theta}) + \boldsymbol{\epsilon}, \quad (7)$$

in which $\boldsymbol{\xi}(\boldsymbol{\omega}; \boldsymbol{\theta})$ is the vector of modal damping ratios predicted using Eq. (5), and $\boldsymbol{\epsilon}$ is the modal damping ratio identification error, which can be assumed to be a random process with a Gaussian distribution having zero mean and a covariance matrix of $\sigma_0^2 \mathbf{I}_{n \times n}$. Hence, we have $p(\hat{\boldsymbol{\xi}}|\boldsymbol{\theta}) \sim N(\boldsymbol{\xi}(\boldsymbol{\omega}; \boldsymbol{\theta}), \sigma_0^2 \mathbf{I}_{n \times n})$, and the posterior PDF, $p(\boldsymbol{\theta}|\hat{\boldsymbol{\xi}})$, could be analytically calculated for a large class of conjugate prior PDFs because modal damping ratios are linear functions of the calibration parameters $\boldsymbol{\theta}$.

The classical Bayesian calibration approach, briefly described above, underestimates the prediction uncertainty because the posterior PDF represents only the estimation uncertainty, which could theoretically reduce to zero in the presence of a large number of data points. To address this issue, similar to our recent study [22], we employ the Embedded Model Error (EME) approach [23] and embed statistical correction into the parameters of the Rayleigh model in order to represent the existing modeling error. Assuming a Gaussian embedding model, we can redefine Rayleigh's coefficients as a Multivariate Normal random variable (MVN), and write

$$\boldsymbol{\theta} = \boldsymbol{\mu} + \mathbf{L}\boldsymbol{\zeta}, \quad (8)$$

where $\boldsymbol{\mu} = [\mu_0, \mu_1]^T$ is the mean, $\boldsymbol{\zeta} = [\zeta_1, \zeta_2]^T$ is an independently and identically distributed random vector with a standard normal distribution, and the matrix \mathbf{L} is a lower-diagonal matrix defined as

$$\mathbf{L} = \begin{bmatrix} \vartheta_{10} & 0 \\ \vartheta_{11} & \vartheta_{21} \end{bmatrix}. \quad (9)$$

Using this embedded model, $\tilde{\boldsymbol{\theta}} = [\mu_0, \mu_1, \vartheta_{10}, \vartheta_{11}, \vartheta_{21}]^T$ is the new parameter vector that must now be estimated. Through this parameter redefinition, the uncertainty in mean would represent the estimation uncertainty caused by identification error and/or lack of data, while the modeling error reserved through the randomness part represented by $\mathbf{L}\boldsymbol{\zeta}$ term.

Based on this redefinition of Rayleigh's coefficients, the data model presented in Eq. (7) can be rewritten as

$$\hat{\boldsymbol{\xi}} = \mathbf{A}\boldsymbol{\mu} + \mathbf{A}\mathbf{L}\boldsymbol{\zeta} + \boldsymbol{\epsilon}, \quad (10)$$

where

$$\mathbf{A} = \begin{bmatrix} \frac{1}{2\omega_1} & \frac{\omega_1}{2} \\ \vdots & \vdots \\ \frac{1}{2\omega_n} & \frac{\omega_n}{2} \end{bmatrix}. \quad (11)$$

Assuming a uniform but bounded prior distribution for unknown parameters to ensure damping ratios are positive, the posterior PDF of the parameters would be proportional to the likelihood function (see Eq. (6)), and can be written using the new data model as:

$$p(\tilde{\boldsymbol{\theta}}|\hat{\boldsymbol{\xi}}) \propto \frac{1}{(2\pi)^{\frac{n}{2}} \sqrt{|\boldsymbol{\Sigma}_{\mathbf{L}} + \sigma_0^2 \mathbf{I}_{n \times n}|}} \exp \left\{ -\frac{1}{2} (\hat{\boldsymbol{\xi}} - \mathbf{A}\boldsymbol{\mu})^T (\boldsymbol{\Sigma}_{\mathbf{L}} + \sigma_0^2 \mathbf{I}_{n \times n})^{-1} (\hat{\boldsymbol{\xi}} - \mathbf{A}\boldsymbol{\mu}) \right\}, \quad (12)$$

where $\boldsymbol{\Sigma}_{\mathbf{L}} = (\mathbf{A}\mathbf{L})(\mathbf{A}\mathbf{L})^T$. Then, Markov Chain Monte Carlo (MCMC) sampling can be used to propagate this posterior PDF through any predictive model (e.g., a Finite Element model for conducting nonlinear time history analysis) to obtain the mean and variance of the prediction. Modal damping ratios are linearly dependent on Rayleigh coefficients (Eq. (5)), so their mean and variance can be calculated directly as

$$\bar{\boldsymbol{\xi}} = \frac{1}{N} \sum_{i=1}^N \mathbf{A}\boldsymbol{\mu}_i, \quad (13)$$

$$\sigma_{\boldsymbol{\xi}}^2 = \frac{1}{N} \sum_{i=1}^N (\mathbf{A}\mathbf{L}_i)(\mathbf{A}\mathbf{L}_i)^T + \frac{1}{N-1} \sum_{i=1}^N (\mathbf{A}\boldsymbol{\mu}_i - \bar{\boldsymbol{\xi}})^2, \quad (14)$$

where $\boldsymbol{\mu}_i$ and \mathbf{L}_i are constructed using MCMC samples of $\tilde{\boldsymbol{\theta}}$. The first term in Eq. (14) represents the contribution of the modeling error to the prediction uncertainty, while the second term is the posterior uncertainty, which is caused by a lack of data.

NUMERICAL EXAMPLE

To illustrate the calibration process and uncertainty propagation, we utilize a simulated example. Consider a 7-DOF shear building model with a uniform mass of $m = 3 \times 10^5$ and a bottom-to-top decreasing inter-story stiffness $k = 5 \times 10^7 [18, 14, 10, 6, 4, 2, 1]$. The natural frequencies of this model are reported in **Table 1**. Two damping scenarios are considered here. In the first scenario, a Rayleigh damping model with $a_0 = 0.5$ and $a_1 = 0.005$ is used to generate modal damping ratios, meaning there is no modeling error. In the second scenario, some arbitrary modal damping ratios are considered, which do not follow any Rayleigh model[§]. These two sets of damping ratios are shown in **Table 1** as well. **Figure 1** displays the damping values of these two models along with 200 Rayleigh model samples constructed by randomly selecting a_0 and a_1 from uniform distributions bounded in $[0.01, 1]$ and $[0.0001, 0.01]$, respectively. In **Figure 1a**, it is possible to find a Rayleigh model sample perfectly representing the data points, while there is no perfect model in **Figure 1b**. We conducted Bayesian calibration with embedded model error for both cases and predicted Rayleigh damping models along with their uncertainties presented in **Figure 2**. In this figure, the mean prediction, $\bar{\boldsymbol{\xi}}(\boldsymbol{\omega})$, is shown in red, and the dark blue area represents one standard deviation, $\sigma_{\boldsymbol{\xi}}(\boldsymbol{\omega})$, around the mean prediction. The posterior uncertainty coming only from the

[§] To have similar plots in Rayleigh and non-Rayleigh cases, a_0 and a_1 in the Rayleigh model are set such that they create a damping model very close to the mean prediction in the non-Rayleigh case.

estimation error (the square root of the second term in Eq. (14)) is shown in light blue. As seen in **Figure 2a**, the prediction is nearly perfect with almost zero uncertainty because the model is accurate and the data is noise-free. However, when the model is not a correct representation of the data (**Figure 2b**), a large model error is estimated and the posterior uncertainty (light blue area) represents a small part of it.

Table 1. Natural frequencies and modal damping ratios of the cases used in this study.

Mode	$f_n = \frac{\omega_n}{2\pi}$ (Hz)	Rayleigh model ξ (%)	Non-Rayleigh model ξ (%)
1	0.79	6.21	4.00
2	1.71	5.08	7.00
3	2.67	5.65	8.00
4	3.76	7.03	5.00
5	5.21	9.06	6.00
6	7.03	11.61	5.00
7	9.64	15.55	20.00

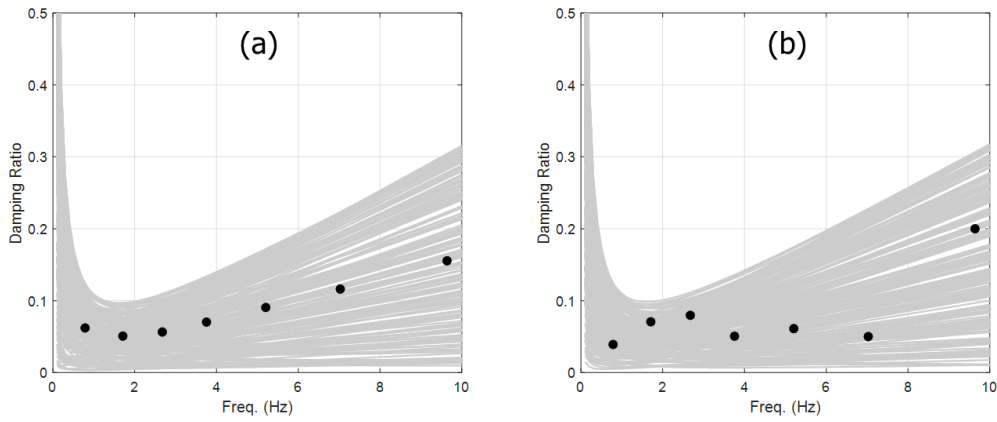


Figure 1. Random samples of the Rayleigh model and modal damping data points for (a) Rayleigh and (b) non-Rayleigh damping data sets.

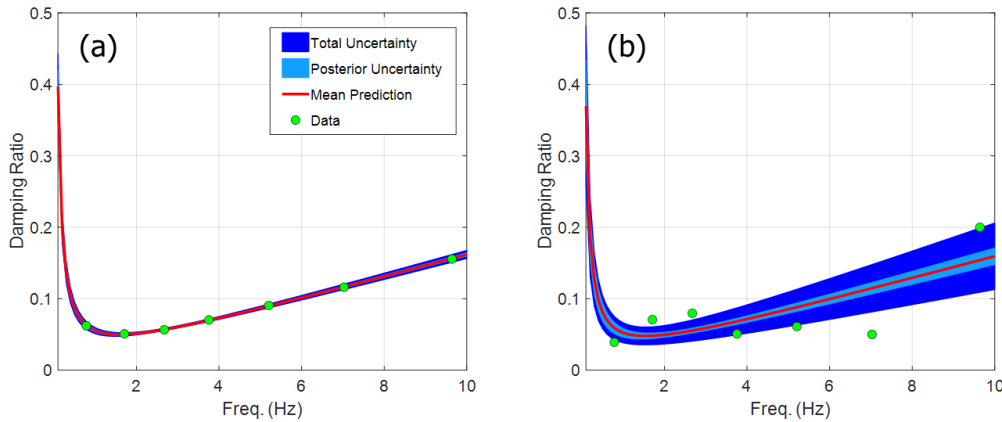


Figure 2. Mean and uncertainty of the damping prediction using (a) Rayleigh and (b) non-Rayleigh damping data.

The marginal and joint PDFs of the estimated Rayleigh coefficients are shown in **Figure 3**. **Figure 3a** shows that when there are no modeling and measurement errors, a_0 and a_1 are estimated very accurately with very small uncertainties (narrow PDFs), while PDFs of the parameters in the second case are wide due to the embedded modeling error (**Figure 3b**).

To demonstrate the effects of damping modeling errors on the dynamic response of the building model, we analyze it under an earthquake ground motion recorded during the 1971 San Fernando earthquake at a free-field station close to the Los Angeles Hollywood Storage building. **Figure 4** shows absolute acceleration of the roof using each of the random Rayleigh responses in red. The deterministic responses obtained using exact modal damping ratios are shown in black. As expected, when the correct damping model (**Figure 4a**) is used, the mean and true responses are very close, and the estimated

uncertainty is negligible. However, as shown in **Figure 4b**, the mean response differs from the true response when an inaccurate damping model is used. Nonetheless, thanks to the proposed embedded model, the predicted uncertainty is able to capture the true response adequately.

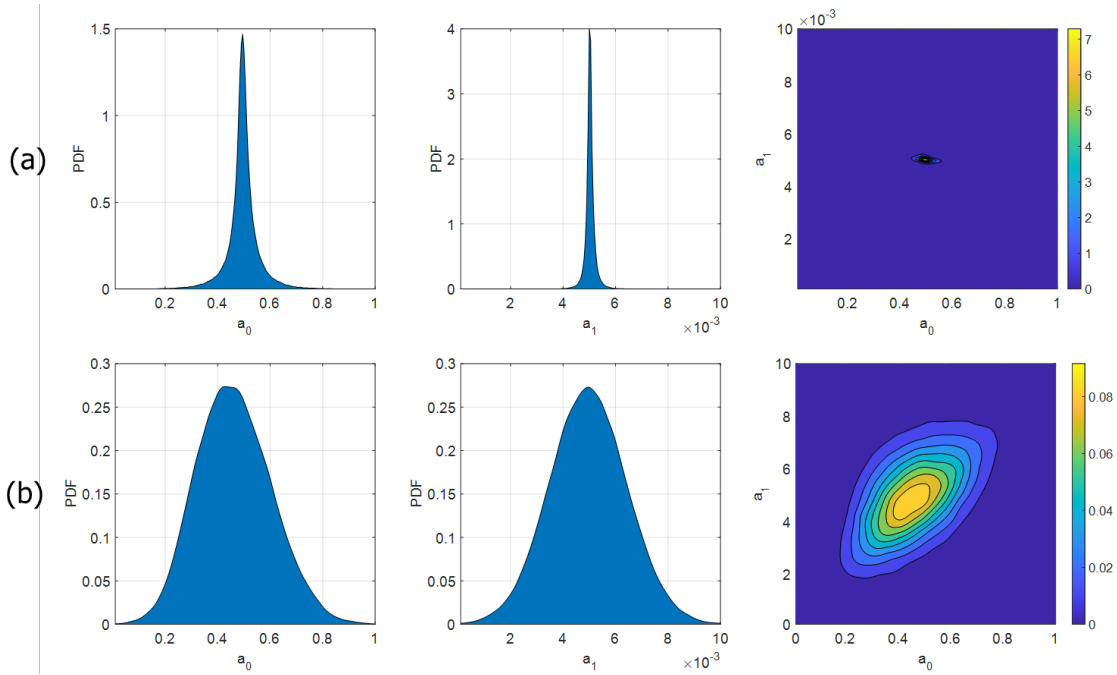


Figure 3. Marginal and joint PDFs of Rayleigh damping coefficients for calibration using (a) Rayleigh and (b) non-Rayleigh damping data.

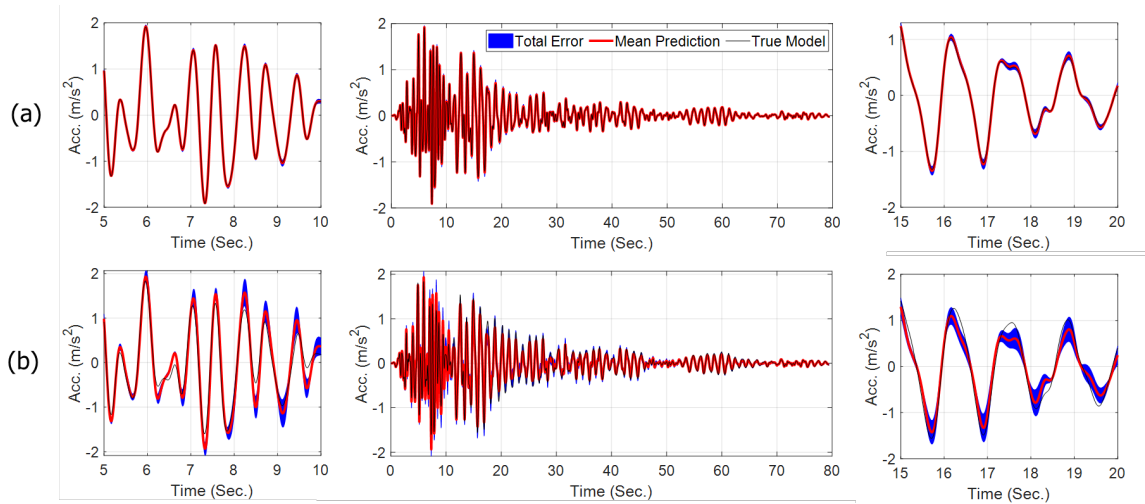


Figure 4. Absolute acceleration time history of the roof calculated using damping models calibrated by (a) Rayleigh and (b) non-Rayleigh damping data.

CONCLUSIONS

This paper introduces a systematic approach to address the uncertainty inherent in the Rayleigh damping model, commonly utilized in structural analyses. By employing a Bayesian calibration with an embedded modeling error, we treat the coefficients of the Rayleigh model as random variables, incorporating modal damping ratios as calibration data. Through a numerical example, we demonstrate the effectiveness of this approach in quantifying and addressing modeling uncertainty associated with the Rayleigh damping model. With this approach, the uncertainty stemming from inaccuracies in the Rayleigh damping model can be quantified for any forward prediction. Naturally, the level of such uncertainty in the predictions would

vary depending on the proximity of the modal damping ratios to a Rayleigh model, the type of structural system, the frequency content of the excitation, and the type of demand parameter of interest.

ACKNOWLEDGMENTS

Sandia National Laboratories is a multimission laboratory managed and operated by National Technology and Engineering Solutions of Sandia, LLC., a wholly owned subsidiary of Honeywell International, Inc., for the U.S. Department of Energy's National Nuclear Security Administration under contract DE-NA-0003525.

REFERENCES

1. Chopra AK. *Dynamics of structures*. vol. 3. Prentice Hall New Jersey; 1995.
2. Taciroglu E, Ghahari SF. *Development of accurate damping models for nonlinear time history analysis*. 2019.
3. Kareem A, Gurley K. Damping in structures: Its evaluation and treatment of uncertainty. *Journal of Wind Engineering and Industrial Aerodynamics* 1996; **59**(2–3). DOI: 10.1016/0167-6105(96)00004-9.
4. Soyoz S, Taciroglu E, Orakcal K, Nigbor R, Skolnik D, Lus H, *et al.* Ambient and Forced Vibration Testing of a Reinforced Concrete Building before and after Its Seismic Retrofitting. *Journal of Structural Engineering* 2013; **139**(10). DOI: 10.1061/(asce)st.1943-541x.0000568.
5. Cruz C, Miranda E. Damping Ratios of the First Mode for the Seismic Analysis of Buildings. *Journal of Structural Engineering* 2021; **147**(1). DOI: 10.1061/(asce)st.1943-541x.0002873.
6. Bernal D, Döhler M, Kojidi SM, Kwan K, Liu Y. First mode damping ratios for buildings. *Earthquake Spectra* 2015; **31**(1): 367–381. DOI: 10.1193/101812EQS311M.
7. Xiang Y, Naeim F, Zareian F. Evaluation of natural periods and modal damping ratios for seismic design of building structures. *Earthquake Spectra* 2020; **36**(2). DOI: 10.1177/8755293019900776.
8. Clough RW, Penzien J. *Dynamics of Structures*. 2013. DOI: 10.1002/9781118599792.
9. W. LR. The Theory of Sound. *Nature* 1898; **58**(1493). DOI: 10.1038/058121a0.
10. Hart GC, Vasudevan R. EARTHQUAKE DESIGN OF BUILDINGS:DAMPING. *ASCE J Struct Div* 1975; **101**(1). DOI: 10.1061/jsdeag.0003964.
11. Cruz C, Miranda E. Evaluation of the Rayleigh damping model for buildings. *Engineering Structures* 2017; **138**. DOI: 10.1016/j.engstruct.2017.02.001.
12. Jehel P. A critical look into Rayleigh damping forces for seismic performance assessment of inelastic structures. *Engineering Structures* 2014; **78**. DOI: 10.1016/j.engstruct.2014.08.003.
13. Erduran E. Evaluation of Rayleigh damping and its influence on engineering demand parameter estimates. *Earthquake Engineering and Structural Dynamics* 2012; **41**(14). DOI: 10.1002/eqe.2164.
14. Chopra AK, McKenna F. Modeling viscous damping in nonlinear response history analysis of buildings for earthquake excitation. *Earthquake Engineering and Structural Dynamics* 2016; **45**(2): 193–211. DOI: 10.1002/eqe.2622.
15. Bernal D. Viscous Damping in Inelastic Structural Response. *Journal of Structural Engineering* 1994; **120**(4): 1240–1254. DOI: 10.1061/(ASCE)0733-9445(1994)120:4(1240).
16. Hall JF. Problems encountered from the use (or misuse) of Rayleigh damping. *Earthquake Engineering and Structural Dynamics* 2006; **35**(5): 525–545. DOI: 10.1002/eqe.541.
17. Luco JE, Lanzani A. Numerical artifacts associated with Rayleigh and modal damping models of inelastic structures with massless coordinates. *Earthquake Engineering & Structural Dynamics* 2019; **48**(13): 1491–1507.
18. CSI S V. 8, 2002. Integrated Finite Element Analysis and Design of Structures Basic Analysis Reference Manual. *Computers and Structures, Inc, Berkeley, California, USA* 2010.
19. McKenna F. OpenSees: a framework for earthquake engineering simulation. *Computing in Science & Engineering* 2011; **13**(4): 58–66.
20. Satake N, Suda K ichi, Arakawa T, Sasaki A, Tamura Y. Damping Evaluation Using Full-Scale Data of Buildings in Japan. *Journal of Structural Engineering* 2003. DOI: 10.1061/(asce)0733-9445(2003)129:4(470).
21. Gokhale D V., Box GEP, Tiao GC. Bayesian Inference in Statistical Analysis. *Biometrics* 1974; **30**(1). DOI: 10.2307/2529631.
22. Ghahari SF, Sargsyan K, Çelebi M., Taciroglu E,. Quantifying modeling uncertainty in simplified beam models for building response prediction. *Structural Control and Health Monitoring* 2022; **29**(11): e3078.
23. Sargsyan K, Huan X, Najm HN. Embedded model error representation for bayesian model calibration. *International Journal for Uncertainty Quantification* 2019; **9**(4).